PAPER

An individual-based model to explore the impact of psychological stress on immune infiltration into tumour spheroids

IOP Publishing Phys. Biol. 21 (2024) 026003 https://doi.org/10.1088/1478-3975/ad221a

Physical Biology

PAPER

RECEIVED
27 July 2023

REVISED
28 November 2023

ACCEPTED FOR PUBLICATION
24 January 2024

PUBLISHED
5 February 2024

An individual-based model to explore the impact of psychological stress on immune infiltration into tumour spheroids

Emma Leschiera[1,2,*], Gheed Al-Hity[3], Melanie S Flint[3], Chandrasekhar Venkataraman[4], Tommaso Lorenzi[5], Luis Almeida[6] and Chloe Audebert[6,7]

[1] Léonard de Vinci Pôle Universitaire, Research Center, 92 916 Paris, La Défense, France
[2] Univ. Bordeaux, CNRS, INRIA, Bordeaux INP, IMB, UMR 5251, F-33400 Talence, France
[3] School of Applied Sciences, University of Brighton, Centre for Stress and Age-related Diseases, Moulsecoomb, Brighton BN2 4GJ, United Kingdom
[4] School of Mathematical and Physical Sciences, University of Sussex, Department of Mathematics, Falmer, Brighton BN1 9QH, United Kingdom
[5] Department of Mathematical Sciences 'G. L. Lagrange', Politecnico di Torino, 10129 Torino, Italy
[6] Sorbonne Université, CNRS, Université de Paris, Laboratoire Jacques-Louis Lions UMR 7598, 75005 Paris, France
[7] Sorbonne Université, CNRS, Institut de biologie Paris-Seine (IBPS), Laboratoire de Biologie Computationnelle et Quantitative UMR 7238, 75005 Paris, France
[*] Author to whom any correspondence should be addressed.

E-mail: emma.leschiera@devinci.fr

Keywords: numerical simulations, immune infiltration, psychological stress, individual-based models, tumour-immune interactions

Supplementary material for this article is available online

Abstract

In recent *in vitro* experiments on co-culture between breast tumour spheroids and activated immune cells, it was observed that the introduction of the stress hormone cortisol resulted in a decreased immune cell infiltration into the spheroids. Moreover, the presence of cortisol deregulated the normal levels of the pro- and anti-inflammatory cytokines IFN-γ and IL-10. We present an individual-based model to explore the interaction dynamics between tumour and immune cells under psychological stress conditions. With our model, we explore the processes underlying the emergence of different levels of immune infiltration, with particular focus on the biological mechanisms regulated by IFN-γ and IL-10. The set-up of numerical simulations is defined to mimic the scenarios considered in the experimental study. Similarly to the experimental quantitative analysis, we compute a score that quantifies the level of immune cell infiltration into the tumour. The results of numerical simulations indicate that the motility of immune cells, their capability to infiltrate through tumour cells, their growth rate and the interplay between these cell parameters can affect the level of immune cell infiltration in different ways. Ultimately, numerical simulations of this model support a deeper understanding of the impact of biological stress-induced mechanisms on immune infiltration.

1. Introduction

The ability of psychological stress to induce immune suppression is widely recognised [1–3], but the mechanisms underlying the effects of psychological stress on the adaptive immune response during tumour progression are not completely understood.

There has been increasing interest in detailing the mechanistic role that psychological stress may play in the context of initiation and progression of cancer. In particular, it has been reported that psychological stress positively influences carcinogenesis through mechanisms that promote proliferation, angiogenesis and metastasis, as well as mechanisms that protect tumour cells from apoptosis [4, 5]. The negative role played by psychological stress on the immune system has also been documented. Using a pre-clinical mouse model, in [6] the authors have shown that psychological stress has a negative impact on T cell numbers and activation, as evidenced by a decrease in the numbers of CD8+ and CD3+CD69+ T cells.

In [7], the authors developed a 3D *in vitro* model to explore the effects of the stress hormone cortisol on immune cell infiltration into tumour spheroids.

Using two independent image-based algorithms, they quantified the effects of cortisol on immune infiltration, which was assessed by counting the number of immune cells within the tumour spheroid boundary. The results from this model recapitulated the conclusions of [6], by showing that cortisol triggered a reduction in immune infiltration levels.

The mixture of cytokines produced in the tumour-microenvironment plays a key role in tumour progression [8]. Pro-inflammatory cytokines that are released in response to infection can inhibit tumour development and progression. Alternatively, tumour cells can produce anti-inflammatory cytokines that promote growth, attenuate apoptosis and facilitate metastasis. In the experiments reported in [7], cortisol downregulated IFN-γ and upregulated IL-10. IFN-γ is a pro-inflammatory cytokine that stimulates immune response, through T cell trafficking in the tumour-microenvironment and infiltration [9, 10], whereas IL-10 is an anti-inflammatory cytokine that inhibits immune response by reducing T cell proliferation [11, 12].

From a biological and medical perspective, it is difficult to investigate the connection between psychological stress, immune infiltration and the underlying molecular and cellular processes. The challenge lies in integrating theoretical and empirical knowledge to achieve a deeper understanding of the mechanisms and factors that contribute to inhibition of the anti-tumour immune response. In this context, mathematical models provide easy and cheap tools towards identifying dependencies between different biological phenomena and how these may affect the efficacy of the immune response on much shorter timescales than laborious and expensive experiments. Different aspects of the interaction dynamics between immune and tumour cells have been studied using different deterministic continuum models formulated as ordinary differential equations [13–16], integro-differential equations [17–19] and partial differential equations (PDEs) [20–23]. These models usually describe the evolution of tumour and immune cell densities that depend on one or more independent variables, usually time and/or space. Such models are defined on the basis of cell population-level phenomenological assumptions, which may limit the amount of biological detail incorporated into the model. By using computational models, such as cellular-automaton (CA) models [24, 25], hybrid PDE-CA models [26, 27] and individual-based models (IBMs) [28–31], a mathematical representation of biological phenomena that are challenging to include in purely continuum models can be achieved. In fact, these models can be posed on a spatial domain, where cells spatially interact with each other according to a defined set of rules, which can collectively generate global emergent behaviours of tumour-immune cell competition.

In [27], we proposed an IBM that describes the earliest stages of tumour-immune competition. In this model, we included cytotoxic T lymphocytes (CTLs) and tumour cells, which interact in a two-dimensional domain under a set of rules describing cell division, migration via chemotaxis, cytotoxic killing of tumour cells by CTLs and immune evasion. However, the model in [27] does not consider the role played by psychological stress in immune infiltration and the influence of pro- and anti-inflammatory cytokines on tumour progression. These aspects are addressed in the present work.

In light of these considerations, and motivated by *in vitro* experimental observations in co-culture between cancer spheroids and immune cells [7], in this paper we develop an IBM to study the effect of psychological stress on immune infiltration. The model builds on our previous work [27] and is calibrated to qualitatively reproduce, *in silico*, the experimental results presented in [7]. As mentioned earlier, in this study the authors found that the introduction of cortisol in the co-culture resulted in a decrease in immune cell infiltration into tumour spheroids, as well as in the alteration of IFN-γ and IL-10 levels. In our model, we assume that cells are exposed to psychological stress, and that this deregulates IFN-γ and IL-10 levels. We explore the processes underlying the emergence of different levels of immune infiltration, with particular focus on biological mechanisms regulated by IFN-γ and IL-10. Based on one of the two image-based algorithms developed in [7] to quantify immune infiltration, in our numerical simulations we compute a score to quantify the effects of psychological stress on immune infiltration.

2. Methods

2.1. Summary of the experimental protocol employed in [7]

A summary of the experimental protocol employed in [7] is provided below (further details can be found in [7]). The mathematical model and numerical simulations will then be implemented accordingly, in order to facilitate comparison with the experiments. A schematic summarising the experimental procedure employed in [7] is displayed in figure 1.

2.1.1. Growth of the spheroids

Spheroids from a murine triple negative 66CL4 breast cancer cell line were generated. It took 4 days for the spheroids to fully form, during which their area increased over time. The cell line was seeded at different densities. The seeding density with the largest area, and with the least variation over 4 days of growth post culturing cells into spheroids, was chosen (cf Group-**1** in figure 1). This was done to ensure that the size of the spheroids remained stable and that changes in the spheroids were due to the infiltration of immune cells.

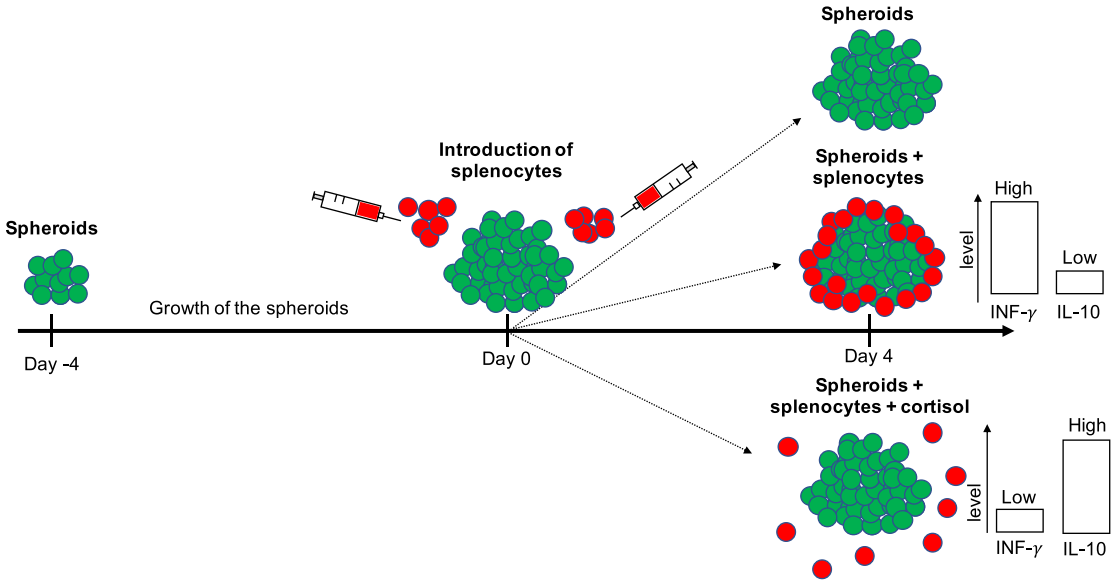

Figure 1. Schematic summarising the experimental protocol employed in [7].

2.1.2. Introduction of splenocytes

After full spheroid generation, immune cells (splenocytes), containing activated T lymphocytes, were co-cultured with spheroids. Cortisol was added to the co-culture and spheroids were later split into different groups. The groups relevant to our study are: Group-**1** containing spheroids only, Group-**2** comprising spheroids and splenocytes, and Group-**3** containing spheroids, splenocytes and cortisol.

2.1.3. Trafficking index measuring infiltration levels of immune cells

To test whether cortisol caused a reduction in immune infiltration in the co-culture, each group was imaged daily for 4 days. From two imaged-based algorithms, two trafficking indices were computed every day to measure immune cell infiltration into the spheroids [7] (i.e. to quantify the number of immune cells within the boundary of the tumour spheroids). Below we report on the implementation of the trafficking index that inspired the development of the score proposed in the present study to measure infiltration levels. Further details can be found in [7].

The *classification-based trafficking index* (TIC) is an algorithm in which first a machine learning algorithm is used to classify each pixel in the image into different groups obtaining three classes: background, tumour cell or immune cell. The TIC is then based on the number of pixels classified as immune cells that are completely surrounded by pixels classified as tumour cells, divided by the total count of pixels surrounded by tumour cells. The resulting statistic yields a number in the interval $[0, 1]$, with a larger TIC indicating a greater level of trafficking.

2.1.4. Investigating the effects of cortisol on immune infiltration

Over 4 days, the co-cultures in Group-**2** and Group-**3** were imaged and the TIC was computed from the corresponding images.

It was found that, compared to the group with untreated spheroids and splenocytes only (i.e. Group-**2**), the introduction of cortisol significantly reduced immune cell infiltration into the spheroids in Group-**3**. Moreover, cortisol significantly reduced IFN-γ levels and increased IL-10 levels.

2.2. Modelling framework

Building upon our previous work [27], to reproduce the *in vitro* results presented in [7], we consider two cell types: tumour cells and immune cells. Although activated immune cells have been considered in the experiments, here we focus on CTLs only. We use a Cellular Potts (CP) approach and the CompuCell3D open-source software [32] to model the interactions between these two cell types.

Adhesive interactions between cells may affect the physical capability of CTLs to infiltrate through tumour cells. In this context, the choice of a CP model is of particular interest, since adhesive interactions between neighboring cells are represented through specific parameters, which describe the net adhesion/repulsion between cell membranes [32] (see supplementary material S1 for a detailed description of the implementation of our CP model).

Moreover, the CompuCell3D software easily allows for the visualisation of the results of numerical simulations. To carry out numerical simulations of the model, we consider both a 2D square spatial domain and a 3D cubic spatial domain.

At each time step, the states of the cells are updated according to the rules described below.

2.2.1. Growth of tumour cells

We denote by $N_T(t)$ the number of tumour cells in the system at time t and we label each cell by an index $n = 1, \ldots, N_T(t)$.

In the experimental setup described in section 2.1.4, spheroids are cultured for a sufficient time until they attain a stable size. To reproduce such dynamics, we let tumour cells proliferate until a maximum tumour size is attained, which corresponds to the carrying capacity of the population. With the selected parameter values, this process takes approximately 7 days.

At the initial time of simulations, we assume a certain number of tumour cells to be tightly packed in a circular configuration positioned at the centre of the domain. At each time-step, tumour cells grow at a rate drawn from a uniform distribution. Mitosis occurs when tumour cells grow to a critical size and then divide. We refer the reader to our previous paper [27] for a detailed description of the modelling strategy employed to represent cell division.

Tumour cells can die due to intra-population competition (i.e. competition between tumour cells for limited space and resources), at a rate proportional to the total number of tumour cells. If tumour cells exhaust their lifespan (which is drawn from a uniform distribution when cells are created) then they die. Dead tumour cells are removed from the domain.

2.2.2. Introduction of CTLs

We denote by $N_C(t)$ the number of CTLs in the system at time t, and we label each of them by an index $m = 1, \ldots, N_C(t)$.

When introduced, CTLs are randomly distributed at the border of the spatial domain. Once in the domain, CTLs grow and divide through mitosis according to rules similar to those used for tumour cells. CTLs die due to intra-population competition (i.e. competition between CTLs for limited space and resources), at a rate proportional to the total number of CTLs. A CTL can also die due to natural death when it reaches the end of its intrinsic lifespan, which is drawn from a uniform distribution when the cell is created.

We assume that tumour cells at the border of the tumour (the region where cytokines and immune cells are more abundant [33]) secrete a chemoattractant. We assume that this chemoattractant represents a mixture of different chemokines (e.g. CXCL9/10/11 [34, 35]) produced by tumour cells and other cells in the tumour micro-environment (e.g. monocytes, endothelial cells, fibroblasts [36]), and that it triggers the movement of CTLs towards tumour cells. A detailed description of the chemoattractant dynamics is given in supplementary material S1. CTLs are assumed to move up the gradient of the chemoattractant towards tumour cells.

According to the experiments, CTLs are activated against tumour cells. Therefore, we suppose that, upon contact, CTLs can induce tumour cell death with a certain probability. We refer to this probability as the 'immune success rate'. If tumour cells satisfy the conditions to be eliminated then they die.

2.2.3. Infiltration score

Similarly to the TIC proposed in [7] to measure immune infiltration, in our work we define an 'infiltration score'. This score allows us to quantify the level of CTL infiltration into the tumour. Provided that there are tumour cells in the domain, we define the infiltration score as the number of CTLs surrounded by tumour cells, divided by the number of tumour cells and CTLs surrounded by tumour cells; that is,

$$I(t) := \frac{\sum_{m=1}^{N_C(t)} \delta_{m \in N_{CS}(t)}}{\sum_{m=1}^{N_C(t)} \delta_{m \in N_{CS}(t)} + \sum_{n=1}^{N_T(t)} \delta_{n \in N_{TS}(t)}}. \quad (2.1)$$

In (2.1), $\delta_{m \in N_{CS}(t)} = 1$ if $m \in N_{CS}(t)$, and $\delta_{m \in N_{CS}(t)} = 0$ otherwise, where $N_{CS}(t)$ denotes the set of indices of CTLs surrounded by tumour cells at time t. Function $\delta_{n \in N_{TS}(t)}$ is defined in a similar way, where $N_{TS}(t)$ denote the set of indices of tumour cells surrounded by tumour cells at time t. In Compucell3D, these terms are handled by using specific functions which track neighbours of every cell (further details can be found in supplementary material S1). Note that $0 \leqslant I(t) \leqslant 1$.

2.2.4. Investigating the effects of psychological stress on immune infiltration

Over 4 days, CTLs move via chemotaxis towards the tumour and infiltrate into it.

In the experiments reported in [7], the spatio-temporal dynamics of cortisol, IFN-γ and IL-10 are not measured. The measurements focus on the level of immune infiltration into tumour spheroids, as well as IFN-γ and IL-10 amounts after 4 days of co-culture. Therefore, to reduce the number of parameters and the complexity of the model, we do not explicitely model the dynamics of cortisol, IFN-γ or IL-10. Through numerical simulations, we investigate the effects of three parameters associated to IFN-γ and IL-10, which we expect to play a key role in determining the infiltration of CTLs into the tumour. These three parameters are: the secretion rate of the chemoattractant by tumour cells, the 'tumour cell-CTL adhesion strength' and the growth rate of CTLs. Below we detail how these three parameters are associated to IFN-γ and IL-10.

It has been shown that IFN-γ induces the stimulation of various chemokines (e.g. CXCL9/10/11) which drive the chemotactic movement of CTLs towards the tumour [9, 34, 35]. Therefore, in our

study, the role of IFN-γ is investigated by varying the secretion rate of the chemoattractant by tumour cells.

Moreover, IFN-γ induces the expression of cellular adhesion molecules (e.g. E-cadherin or ICAM-1), which enhance the infiltration of CTLs into the tumour [37, 38]. Therefore, the role of IFN-γ is also investigated by varying the 'tumour cell-CTL adhesion strength' (TC-CTL adhesion strength). This parameter refers to the CP parameter associated to the adhesion between tumour cell and CTL membranes. In our model, the TC-CTL adhesion strength regulates CTL ability to infiltrate through tumour cells. In particular, high values of this parameter facilitate the infiltration of CTLs through tumour cells, while low values lead the CTLs to accumulate at the margin of the tumour, without infiltrating into it. More details on the calibration of this parameter are provided in supplementary material S2.

Finally, IL-10 is an immunoregulatory cytokine that can attenuate inflammatory responses by suppressing CTL production and proliferation [11, 12]. Therefore, the effect of IL-10 is investigated by varying the growth rate of CTLs.

In this work, we explore different scenarios. We suppose that in non-stressed conditions IFN-γ levels are high, IL-10 levels are low, and CTLs infiltrate into the tumour. In stressed conditions instead, we suppose that IFN-γ levels decrease and IL-10 levels increase, leading to a decreased CTL infiltration. By considering a range of values of these three parameters, we explore their impact on tumour-immune dynamics independently and together, assessing their influence on immune infiltration in a controlled manner.

3. Preliminary results in 2D and 3D

In this section, the results of preliminary numerical simulations of the model in 2D and 3D are presented, which will be used to guide the simulations leading to the main results presented in section 4.

Given the stochastic nature of the model, all the results we present in this section and in section 4 are obtained by averaging over five simulations, which were carried out using the parameter values reported in tables S1 and S2. It should be noted that the standard deviation between these five simulations is relatively small which leads us not to increase the number of simulations (and their relative computational cost). A lower number of replicates would not allow to check the robustness of the results. Full details of model implementation and model parameterisation are provided in supplementary material S1 and supplementary material S2, respectively. Files to run a simulation example of the model with Compucell3D [32] are available at https://plmlab.math.cnrs.fr/leschiera/roleofstress.

3.1. Tumour development in the absence of CTLs

We first establish a preliminary scenario where tumour cells grow, divide and die according to the rules described in section 2.2, in the absence of CTLs. At the initial time of simulations, 35 tumour cells are placed in the domain. More details about the definition of the model initial conditions are given in supplementary material S2. We carry out numerical simulations for 11 days (which we count from day -7 to day 4). The plots in figures 2(a1) and (b1) show the time evolution of the tumour cell number in 2D and 3D, while figures 2(a2), (a3), (b2) and (b3) display samples of initial and final spatial distributions of tumour cells 2D and 3D, respectively. The tumour growth is of logistic type, as expected due to the rules that govern tumour cell division and death. In more detail, as shown by figures 2(a1) and (b1), the number of tumour cells increases from day -7 to day 0. Around day 0, it reaches the carrying capacity. The number of tumour cells at carrying capacity is similar to the seeding density chosen in [7] (cf figure 1 for 66CL4 spheroids in [7]). From day 0 to day 4, the tumour cell number fluctuates around the carrying capacity.

These simulations allowed us to calibrate the model parameters related to tumour cells in order to qualitatively reproduce the growth of the spheroids obtained in the experiments. The other simulations were carried out keeping the values of these parameters fixed and equal to those used for these simulations.

3.2. Control scenario: CTL infiltration in non-stressed conditions

In the experimental results presented by [7], in the absence of cortisol, immune cells are able to infiltrate the tumour spheroids. Here we verify the ability of our model to reproduce such dynamics by exploring the infiltration of CTLs into the tumour over 4 days. For these simulations, the initial number of tumour cells is set at carrying capacity, whereas 150 CTLs are introduced in the domain. The values of the parameters related to CTLs are chosen so as to qualitatively reproduce the interaction dynamics between spheroids and immune cells in non-stressed conditions presented in [7]. The parameters related to IFN-γ and IL-10 levels are set to baseline values (i.e. non-stressed conditions). In particular, we let tumour cells secrete the chemoattractant at a high rate, CTLs grow at their normal rate and display a high capability to infiltrate the tumour cell population (i.e. we consider a sufficiently high value for the TC-CTL adhesion strength). In order to gain a deeper understanding of the effects produced by the three aforementioned parameters on immune infiltration, for the moment we simplify our model by assuming that CTLs are not able to eliminate tumour cells (i.e. the immune success rate is set

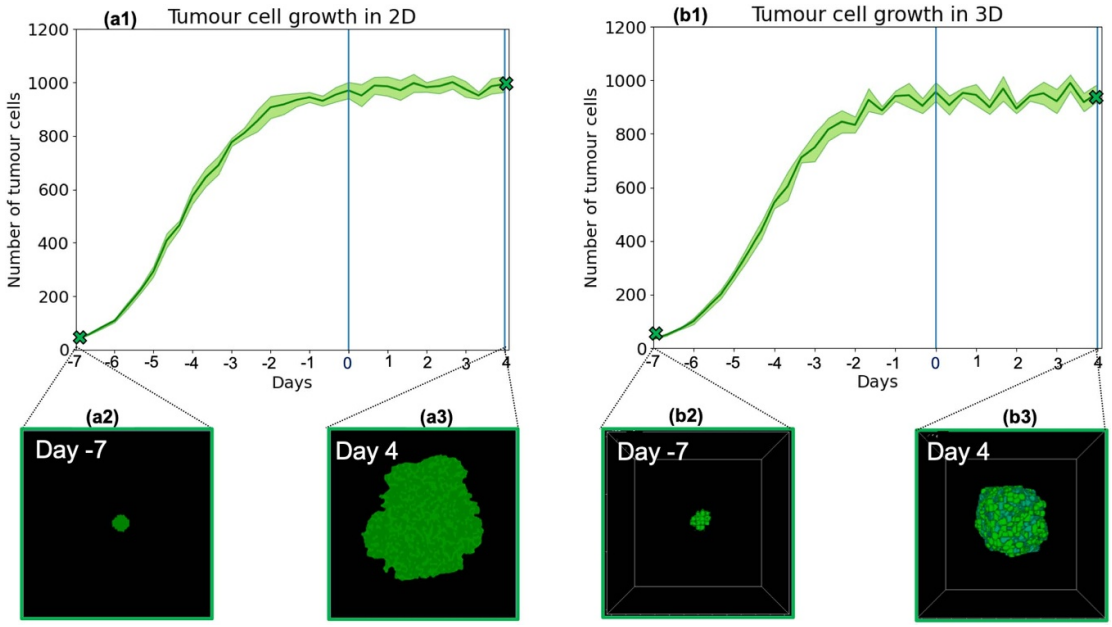

Figure 2. Tumour development in the absence of CTLs. Panels (a1) and (b1) display the time evolution of the tumour cell number in the absence of CTLs in 2D and 3D, respectively. These results correspond to the average over five simulations and the shaded areas indicate $+/-$ standard deviation. Panels (a2), (a3) and (b2), (b3) display samples of the initial and final spatial distributions of tumour cells in 2D and 3D, respectively. The parameter values used to carry out numerical simulations are provided in tables S1 and S2.

equal to 0). The full model with an immune success rate greater than 0 will be considered in section 4.4.

The plots in figures 3(a1) and (b1) show the time evolution of the number of tumour cells and CTLs in 2D and 3D, while figures 3(a2), (a3), (b2) and (b3) display samples of initial and final spatial distributions of tumour cells and CTLs in 2D and 3D, respectively. The choice of parameter values corresponding to these figures results in the infiltration of CTLs into the tumour. The plots in figures 3(c) and (d) display, respectively, the corresponding average value of the infiltration score, computed via (2.1), and the average number of infiltrated CTLs over 4 days. Both in 2D and 3D, as soon as CTLs are introduced in the domain, they move towards the tumour and infiltrate it. Figure 3(c) indicates that the infiltration score increases over time, both in 2D and 3D. In 2D its value tends to saturate between day 3 and day 4. Moreover, the value of the infiltration score in the 3D setting is larger than in the 2D case. Note that, in 2D, the mean value of the infiltration score obtained at day 4 of simulations is similar to the mean value of the TIC computed in [7], when cortisol was not introduced in the co-culture (cf figure 5 in [7]). Figure 3(d) demonstrates that, in 2D, most of the CTLs infiltrate the tumour already at day 1, as the average number of infiltrated CTLs increases only slightly between day 1 and 4. On the other hand, in 3D, CTLs seem to be slightly slower in moving towards the tumour. However, the average number of infiltrated CTLs at the end of numerical simulations is similar in the two settings. Finally, as shown by figures 3(a1) and (b1), and as expected on the basis of the rules that govern tumour cell and CTL growth and death, both in 2D and 3D, over time the number of tumour cells fluctuates around the carrying capacity, while CTL number increases until it reaches a saturation value. This result indicates that the changes in the tumour surface and volume observed in figures 3(a3) and (b3) are due to the infiltration of CTLs into the tumour.

4. Main results

In this section we explore the effects of psychological stress on immune infiltration. To do so, first we decrease the secretion rate of the chemoattractant and the TC-CTL adhesion strength. These two parameters are associated with decreased levels of IFN-γ. Next, for each scenario considered, we decrease the growth rate of CTLs, which is associated with increased levels of IL-10. The initial number and position of tumour cells and CTLs is kept equal to that used in the control scenario.

Conducting baseline numerical simulations in 3D provided valuable insights into potential disparities between calculating the infiltration score on 2D and 3D images. Nevertheless, since in the experiments reported in [7] the infiltration score is computed on 2D images, we now carry out 2D simulations only, also because they require much less computational time than the corresponding 3D simulations.

In this section, we report on results obtained by varying the values of the three aforementioned parameters while the other parameters are kept equal to

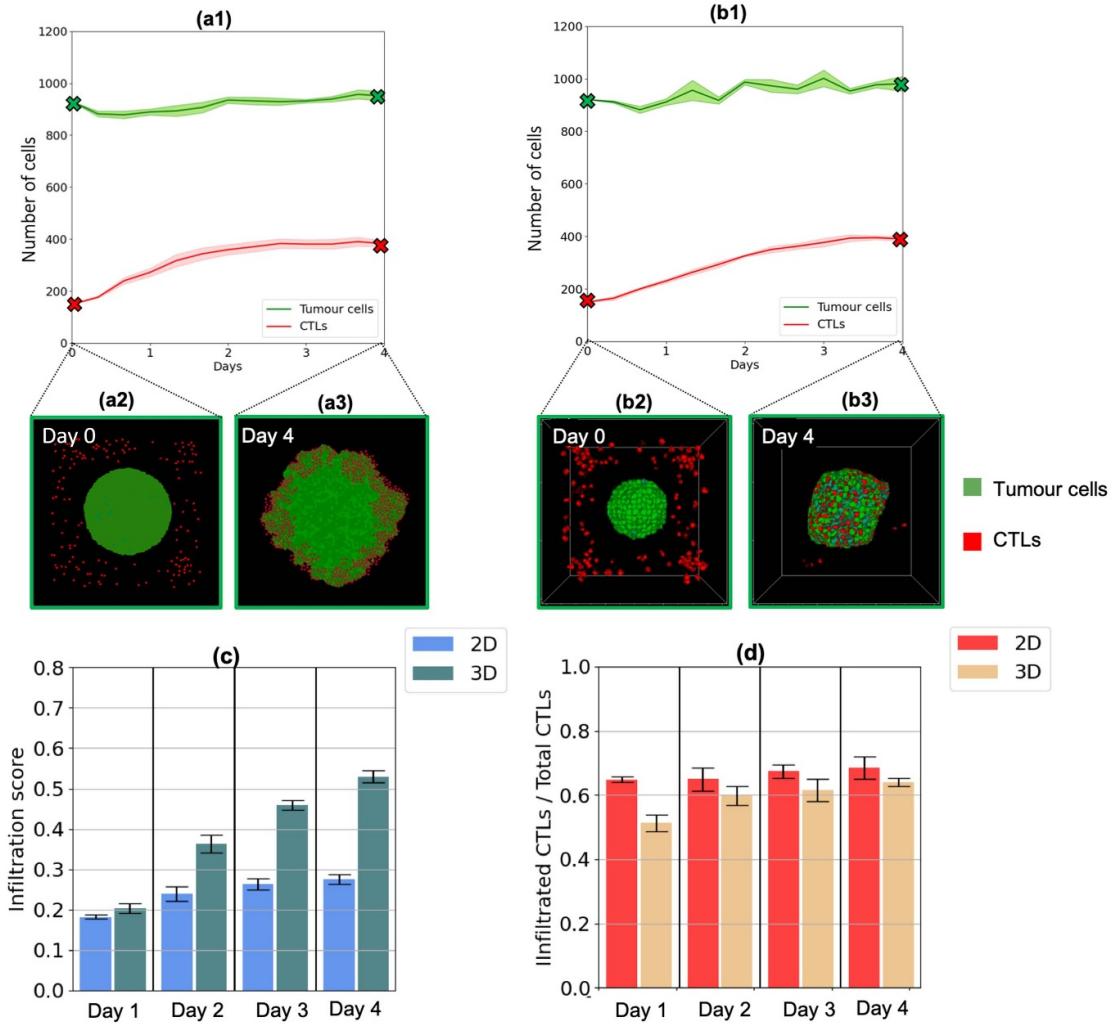

Figure 3. Control scenario: CTL infiltration in non-stressed conditions. Panel (a1) and (b1) display, respectively, the time evolution of the numbers of tumour cells (in green) and CTLs (in red) in 2D and 3D for a choice of parameter values that results in the infiltration of CTLs into the tumour. These results correspond to the average over five simulations and the shaded area indicates $+/-$ standard deviation. Panels (a2), (a3) and (b2), (b3) display samples of the initial and final spatial distribution of tumour cells (in green) and CTLs (in red) in 2D and 3D, respectively. Panel (c) displays the corresponding average value of the infiltration score, computed via (2.1), at different times of the 2D and 3D simulations. The error lines represent the standard deviation between five simulations. Panel (d) displays the ratio between the corresponding average number of infiltrated CTLs and the total number of CTLs at the end of 2D and 3D simulations. The error lines represent the standard deviation between five simulations. The parameter values used to carry out numerical simulations are provided in tables S1 and S2.

the values used in the previous section. For each scenario, the infiltration score is computed via (2.1).

4.1. Decreasing the secretion rate of the chemoattractant and the TC-CTL adhesion strength reduces the infiltration of CTLs into the tumour

To investigate how immune infiltration is affected by IFN-γ levels in the domain, we start by comparing the control scenario of section 3.2 with scenarios in which the values of the secretion rate of the chemoattractant and of the TC-CTL adhesion strength are reduced (cf tables S1 and S2).

Figure 4(a) displays the average value of the infiltration score at different times of the simulations, for high, intermediate and low values of the secretion rate of the chemoattractant and the TC-CTL adhesion strength. This figure shows that both parameters affect the infiltration of CTLs into the tumour, as the infiltration score decreases as soon as one of the two parameters is reduced. In addition, when the TC-CTL adhesion strength is sufficiently high, decreasing the secretion rate of the chemoattractant considerably reduces the infiltration score. On the other hand, for sufficiently low values of the TC-CTL adhesion strength, decreasing the secretion rate of the chemoattractant does not have an impact on the infiltration score, as its value is already small. Taken together, these results suggest that the secretion rate of the chemoattractant has an impact on T cell infiltration only when CTLs display a sufficiently high capability to infiltrate through tumour cells.

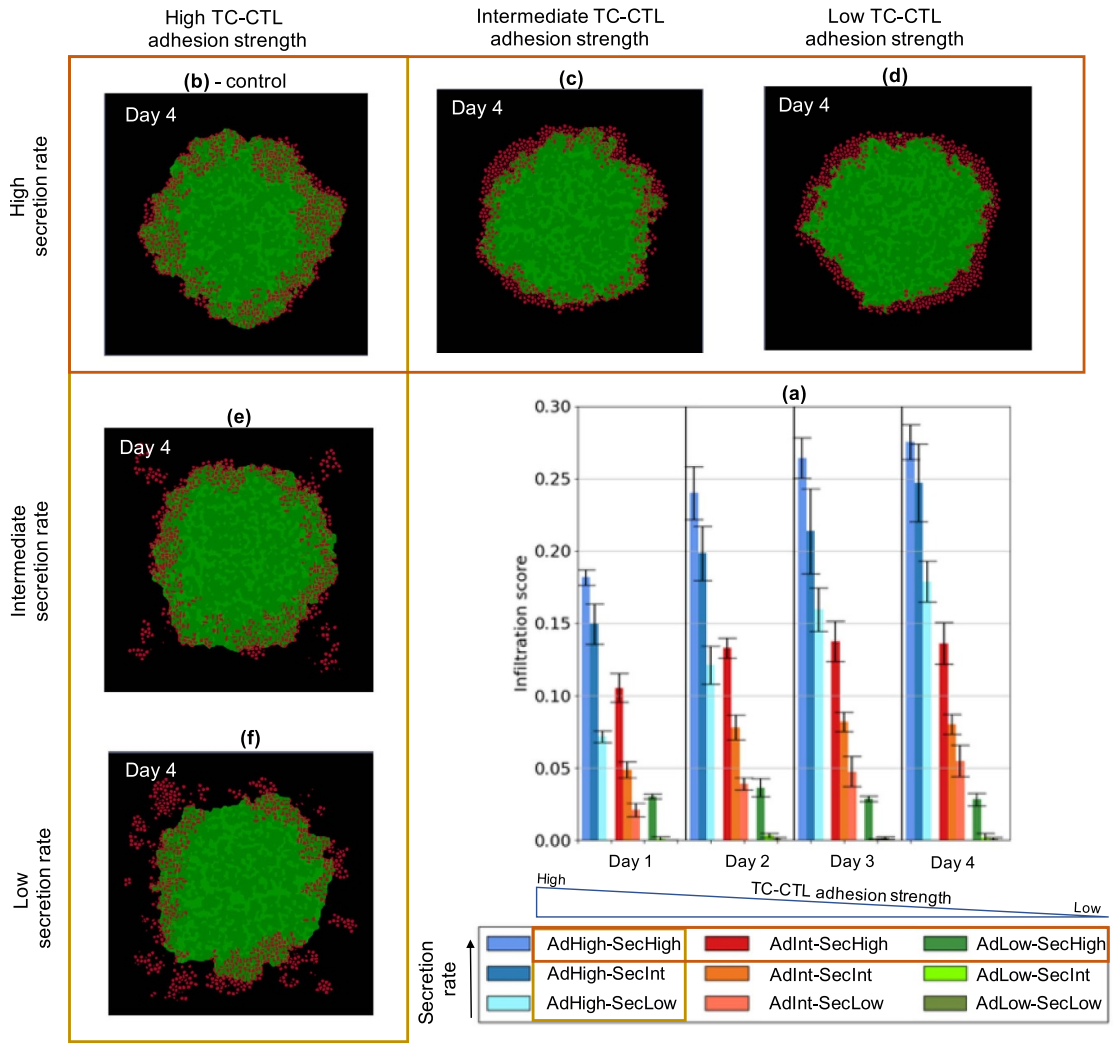

Figure 4. Decreasing the secretion rate of the chemoattractant and the TC-CTL adhesion strength reduces the infiltration of CTLs into the tumour. Panel (a) displays the average value of the infiltration score, computed via (2.1), for different values of the secretion rate of the chemoattractant and the TC-CTL adhesion strength, at different times of the simulations. The error lines represent the standard deviation between five simulations. Panel (b) displays a sample of the final spatial distribution of tumour cells (in green) and CTLs (in red) for the parameter values considered in the control scenario. Panels (c) and (d) display similar plots for two different values of the TC-CTL adhesion strength. Panels (e)–(f) display similar plots for two different values of the secretion rate of the chemoattractant. The parameter values used to carry out numerical simulations are provided in tables S1 and S2.

Then, we analyse the spatial cell distributions observed at the end of simulations. Figures 4(c) and (d) show samples of the final spatial distributions of tumour cells and CTLs for intermediate and low values of the TC-CTL adhesion strength. Figures 4(e) and (f) show similar plots for intermediate and low values of the secretion rate of the chemoattractant. These plots are to be compared with the one in figure 4(b), which displays the final spatial distributions of tumour cells and CTLs obtained in the control scenario. In particular, figures 4(b) and (d) show that decreasing the TC-CTL adhesion strength leads to scenarios in which CTLs accumulate around the tumour, because the secretion rate of the chemoattractant is high, but they do not infiltrate into it. The calculation of the infiltration score defined via (2.1) only takes into account CTLs infiltrated into the tumour but not the ones surrounding it. Therefore, the infiltration score decreases. On the other hand, figures 4(b)–(f) indicate that decreasing the secretion rate of the chemoattractant leads to scenarios in which CTLs away from the tumour are not sensitive to the gradient of the chemoattractant and, therefore, do not move towards the tumour. The more CTLs are not sensitive to the chemoattractant and do not infiltrate the tumour, the more the infiltration score decreases.

Taken together, these results qualitatively reproduce key experimental findings presented in [7], which indicated that cortisol reduced IFN-γ levels

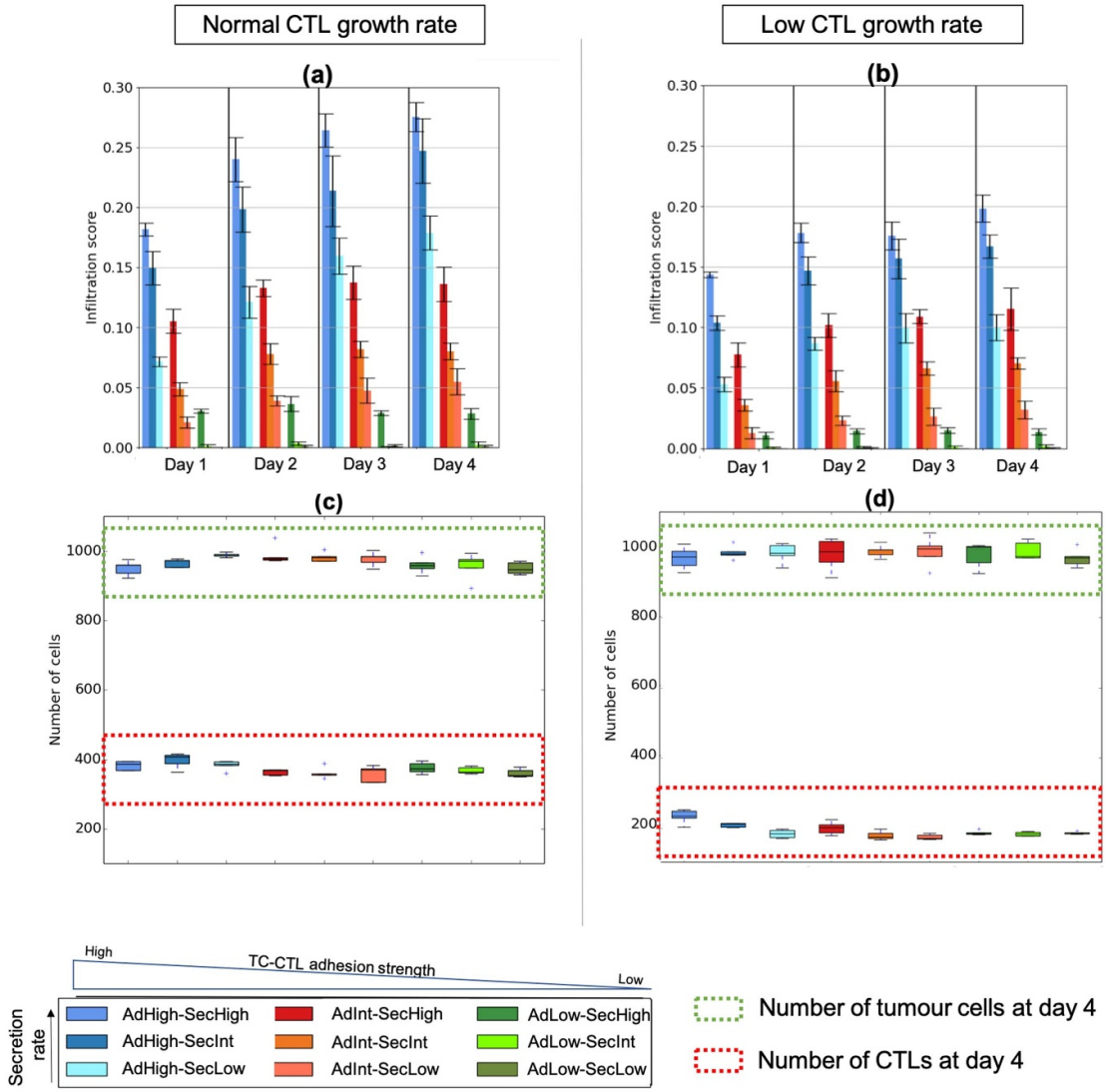

Figure 5. Decreasing the growth rate of CTLs reduces the number of infiltrated CTLs. Plots in panels (a) and (b) display the average value of the infiltration score, computed via (2.1), for different values of the secretion rate of the chemoattractant and the TC-CTL adhesion strength, and at different times of the simulations. In panel (a) CTLs grow at their normal rate, while their growth rate is decreased in panel (b). The error lines represent the standard deviation between five simulations. Panels (c) and (d) display the corresponding number of tumour cells and CTLs at the end of simulations (corresponding to day 4 of the experiments). The parameter values used to carry out numerical simulations are provided in tables S1 and S2.

and led also immune infiltration to reduce. The modelling assumption underlying these computational results may provide the following theoretical explanation for such behaviour. Since IFN-γ may affect both CTL movement and infiltration capabilities, deregulation of IFN-γ levels inhibits CTL ability to migrate towards the tumour and to infiltrate through tumour cells. The interplay between these mechanisms results in a progressive reduction of immune infiltration levels.

4.2. Decreasing the growth rate of CTLs reduces the number of infiltrated CTLs

We further investigate the effects of psychological stress on immune infiltration by exploring the role played by IL-10. For these simulations, we consider the same parameter values used in the previous subsection but we reduce the value of the growth rate of CTLs (cf tables S1 and S2).

Figures 5(a) and (b) show a comparison between the infiltration score obtained when the effects of IL-10 are not considered (i.e. for a normal value of the CTL growth rate), and the one obtained when the effects of IL-10 are considered (i.e. when the CTL growth rate is reduced). Figures 5(c) and (d) also compare the number of tumour cells and CTLs at the end of numerical simulations (i.e. at day 4 of the experiments) for the two scenarios considered. Comparing the results of figure 5(a) with those displayed in figure 5(b), we see that, similarly to the results observed in the previous subsection, decreasing the growth rate of CTLs reduces the

infiltration score only when the TC-CTL adhesion strength is sufficiently high. However, when the TC-CTL adhesion strength is sufficiently low, decreasing the growth rate of CTLs does not have an impact on the infiltration score, as its value is already small. As shown by figures 5(c) and (d), decreasing the growth rate of CTLs leads to a decreased number of CTLs at the end of simulations, while the final number of tumour cells remains similar in the two scenarios.

If we assume that high levels of IL-10 inhibit CTL growth, the outputs of our model indicate that, as expected, decreasing the proliferation rate of CTLs diminishes the number of CTLs in the domain. Moreover, if CTLs display a sufficiently high capability to infiltrate through tumour cells, we observe a reduction in the number of infiltrated CTLs (i.e. the infiltration score decreases). On the other hand, if CTLs have a low capability to infiltrate through tumour cells, decreasing the proliferation rate of CTLs does not affect the infiltration score, as the number of infiltrated CTLs is already low. This suggests that high levels of IL-10 decrease immune infiltration only when CTLs display a sufficiently high capability to infiltrate through tumour cells, that is, when IFN-γ levels are sufficiently high.

4.3. Relationship between IFN-γ and IL-10 levels and infiltration score

The results presented in the previous subsections summarise how scenarios corresponding to different levels of CTL infiltration into the tumour can emerge under sample combinations of the values of the secretion rate of the chemoattractant, the TC-CTL adhesion strength and the CTL growth rate. We now undertake a more comprehensive investigation of the relationship between these parameters and the infiltration score.

In order to do this, we perform numerical simulations holding all parameters constant but considering a broader range of values of the secretion rate of the chemoattractant by tumour cells, the tumour cell-CTL adhesion strength and the growth rate of CTLs. For each pair of parameters, the third parameter is set to its baseline value. For each scenario considered, we determine the final value of the infiltration score computed via (2.1). The results obtained are summarised in the heat maps of figure 6.

As shown by the green regions on the bottom side of the two heat maps of figures 6(a) and (b), for sufficiently small values of the tumour cell-CTL adhesion strength, the immunoscore is relatively low (<0.1) independently of the value of the chemoattractant secretion rate and the CTL growth rate. This is due to the fact that, independently of their number or their sensitivity to the chemoattractant, CTLs accumulate around the tumour, but they might not infiltrate into it. On the other hand, when low values of the chemoattractant secretion rate and the growth rate of CTLs are considered, but the baseline (i.e. high) value of the tumour cell-CTL adhesion strength is considered (cf figure 6(c)), the infiltration score is larger than in the two previous scenarios.

The orange-red regions of the heat maps of figure 6. indicate that there are several possible parameter ranges giving rise to an intermediate infiltration score (between 0.1 and 0.2). The first and second ones correspond to intermediate values of the tumour cell-CTL adhesion strength along with either intermediate to low values of the chemoattractant secretion rate (cf figure 6(a)) or normal to low values of the CTL growth rate (cf figure 6(b)). The third parameter range corresponds to low to normal values of the CTL growth rate along with intermediate to low values of the chemoattractant secretion rate (cf figure 6(c)).

Finally, as shown by the light blue regions on the top-left side of figures 6(a) and (b), for high values of the three parameters, which correspond to the baseline parameters chosen in the control scenario, the value of the immunoscore is relatively high (>0.2). Figure 6(c) shows that a relatively high immunoscore can be obtained also for lower values of the CTL growth rate (resp. chemoattractant secretion rate), provided that the chemoattractant secretion rate (resp. CTL growth rate) is large enough. Moreover, these results also show that increasing the growth rate of CTLs or the chemoattractant secretion rate to values higher than those considered in the control scenario does not always increase the infiltration score.

4.4. Increasing the immune success rate has an impact on the infiltration score only when the TC-CTL adhesion strength is sufficiently large

So far, we have investigated with our model the effects of psychological stress on immune infiltration in the case where CTLs are not able to eliminate tumour cells. However, in [7] is reported that immune cells are activated against the spheroids, although the cytotoxic effect of immune cells on tumour cells is not particularly pronounced. Motivated by these considerations, now we investigate tumour-immune dynamics and the effects of psychological stress on immune infiltration in the case where CTLs can eliminate tumour cells with a small probability.

Figures 7(a) and (b) show a comparison between the infiltration score obtained with the parameter values considered in section 4.1, assuming that CTLs are able, or not able, to eliminate tumour cells (i.e. the

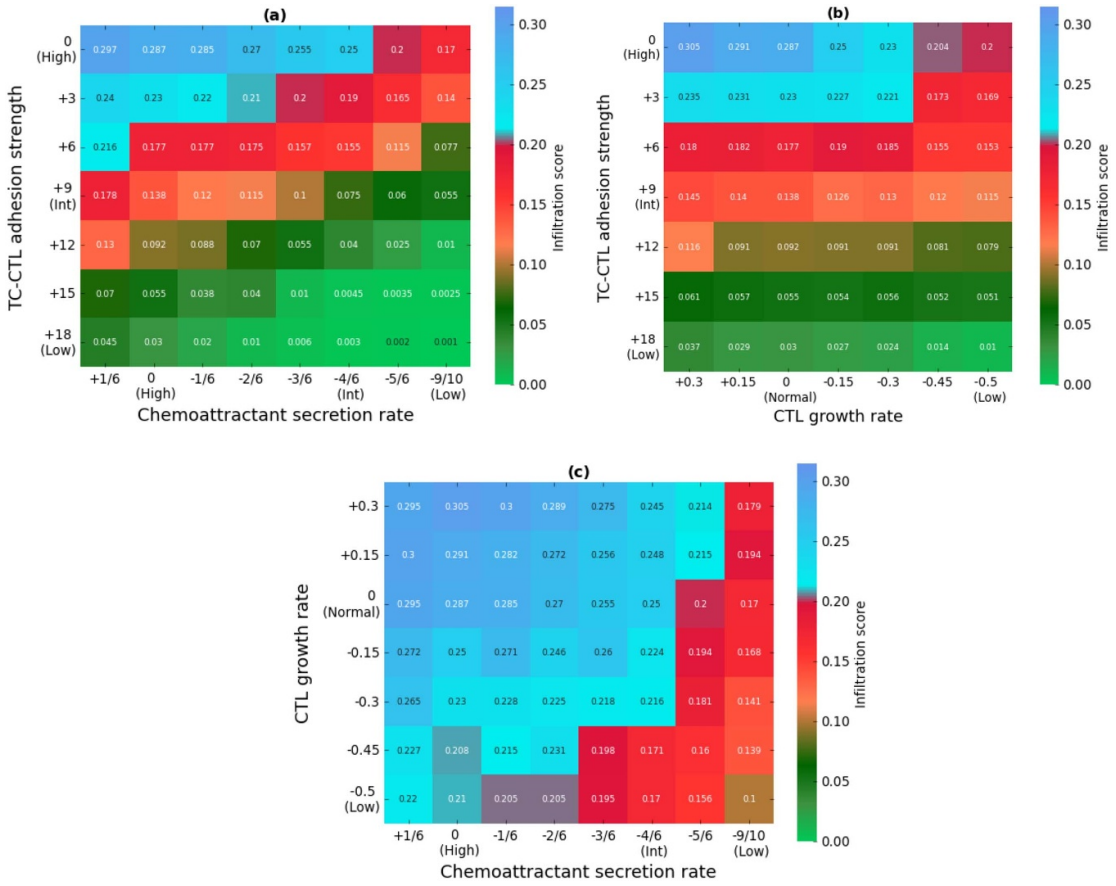

Figure 6. Relationship between IFN-γ and IL-10 levels and infiltration score. Panel (a) displays the average value of the infiltration score, computed via (2.1), for different values of the secretion rate of the chemoattractant and the TC-CTL adhesion strength at the end of the simulations. Panel (b) displays a similar plot for different values of the TC-CTL adhesion strength and the CTL growth rate. Panel (c) displays a similar plot for different values of the secretion rate of the chemoattractant and the CTL growth rate. Results are shown for variations of: $+\frac{1}{6}, -\frac{1}{6}, -\frac{2}{6}, -\frac{3}{6}$ (cf Int), $-\frac{4}{6}, -\frac{5}{6}, -\frac{9}{10}$ (cf Low) from the baseline (cf High) value of the secretion rate of the chemoattractant; $+3, +6, +9$ (cf Int), $+12, +15, +18$ (cf Low) from the baseline (cf High) value of the TC-CTL adhesion strength; $+0.3, +0.15, -0.15, -0.3, -0.45, -0.5$ (cf Low) from the baseline (cf Normal) value of the CTL growth rate. For each pair of parameters, the value of the third parameter is set to its baseline value. The parameter values used to carry out numerical simulations are provided in tables S1 and S2.

immune success rate is either zero or different from zero—cf table S2). Figures 7(c) and (d) show a comparison between the number of tumour cells and CTLs at the end of simulations (corresponding to day 4 of the experiments) for the two scenarios considered. Comparing the results of figure 7(a) with those displayed in figure 7(b), we see that, when the TC-CTL adhesion strength is sufficiently high, increasing the immune success rate decreases the infiltration score. This is probably due to the fact that, when CTLs can infiltrate through tumour cells, they are more likely to come into contact with tumour cells, thus increasing the chance for CTLs to eliminate them. Since dead tumour cells are cleared from the domain, this in turn diminishes the number of CTLs surrounded by tumour cells, leading to a reduced infiltration score. However, when the TC-CTL adhesion strength is sufficiently low, increasing the immune success rate does not have an impact on the infiltration score. In fact, in this scenario, CTLs accumulate around the tumour, decreasing their probability to come into contact with tumour cells. This reduces their chance to eliminate tumour cells. Analogous considerations hold for the case in which lower growth rates of CTLs are considered (results not shown).

As shown by figures 7(c) and (d), increasing the immune success rate leads to a slightly decreased number of tumour cells at the end of simulations only when sufficiently large values of the TC-CTL adhesion strength and the secretion rate of the chemoattractant are considered. On the other hand, for intermediate and sufficiently small values of these two parameters, increasing the immune success rate does not have an impact on the final number of tumour cells.

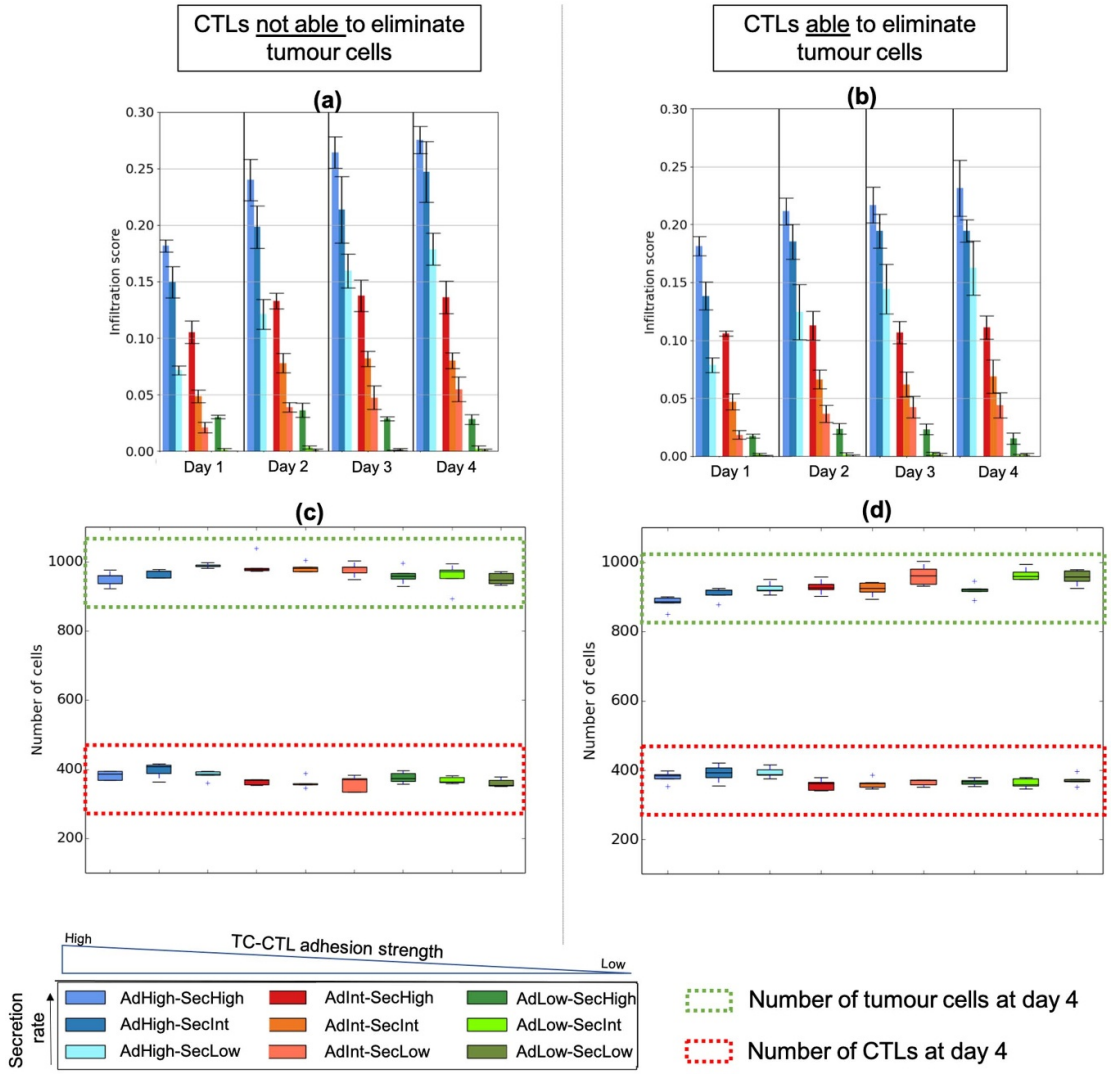

Figure 7. Increasing the immune success rate has an impact on the infiltration score only when the TC-CTL adhesion strength is sufficiently large. Panels (a) and (b) displays the average value of the infiltration score, computed via (2.1), for different values of the secretion rate of the chemoattractant and the TC-CTL adhesion strength, and at different times of the simulations. In panel (a) CTLs are assumed not to be able to eliminate tumour cells, while they are assumed to be able to eliminate them in panel (b). Panels (c) and (d) display the corresponding number of tumour cells and CTLs at the end of simulations (corresponding to day 4 of the experiments). The parameter values used to carry out numerical simulations are provided in tables S1 and S2.

5. Discussion, conclusions and research perspectives

The *in vitro* co-culture experiments presented in [7] are performed in an isolated and relatively homogeneous environment and involve only a few constituents: tumour spheroids, activated immune cells, culture medium and cortisol. Furthermore, each experiment has clear observables, namely the confocal images of the co-culture, the trafficking indices and the levels of IFN-γ and IL-10, which make these experiments highly suitable to be studied through a mathematical model.

In this paper, we have presented an IBM to describe the interaction dynamics between CTLs and tumour cells, to reproduce qualitative aspects presented in [7] and evaluate immune cell trafficking into tumour cells under normal and stressed conditions. In particular, on the basis of the experiments presented in [7], we have investigated in a causal, systematic manner the way in which IFN-γ and IL-10 may impact on the infiltration of CTLs into tumour cells.

The results of numerical simulations qualitatively reproduce, both in 2D and 3D, the growth of the tumour spheroids prior the introduction of immune cells and the tumour-immune dynamics in non-stressed conditions. The tumour growth is of logistic type. In the control scenario, i.e. the scenario in which the secretion rate of the chemoattractant, the TC-CTL adhesion strength and the CTLs growth rate are set at their baseline values, CTLs are able to infiltrate into the tumour.

We then have investigated the effects of psychological stress on immune infiltration. First, the results of our model support the idea that reducing the secretion rate of the chemoattractant and the TC-CTL

adhesion strength, which are associated to a decrease in IFN-γ levels, reduces the infiltration of CTLs into the tumour. These results also suggest that the secretion rate of the chemoattractant is more likely to have an impact on T cell infiltration when CTLs display a sufficiently high capability to infiltrate through tumour cells. We have also studied the effects of psychological stress on immune infiltration by reducing the growth rate of CTLs, which is associated to increased IL-10 levels. Decreasing the growth rate of CTLs reduces the number of CTLs in the domain. This leads to a significant reduction in the infiltration score only when the TC-CTL adhesion strength is sufficiently large. The sensitivity analysis of these three paramaters has allowed us to undertake a more comprehensive investigation of the relationship between them and the value of the infiltration score. Finally, we have performed numerical simulations by letting CTLs eliminate tumour cells with a small probability - i.e. when the immune success rate is greater than 0. In the scenario in which CTLs are able to infiltrate into the tumour, increasing the immune success rate leads to a reduced infiltration score, as tumour cells in contact with CTLs are eliminated. This in turn leads to a slightly decreased number of tumour cells at the end of simulations.

In summary, the results of numerical simulations of our model indicate that the interplay between IFN-γ and IL-10 plays a key role in determining the effects of psychological stress on immune infiltration reported in [7], as both cytokines contribute to regulate immune infiltration in opposite ways. Moreover, our results shed light on the impact of three biological stress-induced mechanisms on immune infiltration. In particular, they support the idea that a high infiltration score can be obtained only when the secretion rate of the chemoattractant and the TC-CTL adhesion strength are large, provided that the growth of CTLs is not inhibited. On the other hand, reducing the value of these parameters can lead to a reduced immune infiltration in different ways. For example, we found that the parameter having the strongest impact on immune infiltration is the TC-CTL adhesion strength, which is associated with the physical capability of CTLs to infiltrate through tumour cells. In this regard, the development of abnormal structural features that inhibit the ability of CTLs to penetrate tumour sites is a hallmark of cancer progression [34]. Evidence is emerging that glucocorticoids act on adhesion of immune cells by inhibiting adhesion molecules (integrins and selectins) [39, 40]. The deregulation of adhesion molecules may act as barriers to T cell migration and infiltration. In this context, the results of this study support the idea that new glucocorticoid receptor antagonists should be developed to target cell adhesion molecules in order to enhance immune infiltration.

The results of numerical simulations also support the idea that an efficient anti-tumour immune response can occur only in highly infiltrated tumours. This is a key result because it indicates that therapeutic strategies promoting the infiltration of CTLs into tumours may be a promising approach against cancer. In particular, our findings suggest that a synergistic effect can be achieved by combining glucocorticoid receptor antagonists, which facilitate CTL infiltration, with immune checkpoint therapies, which enhance the effectiveness of *in situ* anti-tumour immune response [34].

The current version of our model can be developed further in several ways. Firstly, due to the high computational cost in simulating the three dimensional version of our model, we carried out 3D simulations only to part of our study. However, by running the simulations on high performance computers, this limitation may be addressed in the future and a larger spectrum of parameter values could be tested.

We managed to calibrate some parameters of the model (see tables S1 and S2) from the literature and define them on the basis of precise biological assumptions. However, there are some parameters (e.g. parameters related to the dynamics of the chemoattractant, the death rate of tumour and CTLs due to intra-population competition) whose values were simply chosen with an exploratory aim and to qualitatively reproduce essential aspects of the experimental results obtained in [7]. In order to minimise the impact of this limitation on the conclusions of our study, first we selected a baseline set of parameters that allowed to reproduce the growth of the spheroids and CTL infiltration as obtained in [7]. Then, we carried out simulations by keeping all parameter fixed and changing only the values of our three parameters of interest, and then comparing the simulation results so obtained.

To keep the model as simple as possible, we chose to include only mechanisms that were necessary to reproduce part of the experimental results presented in [7]. If experimental measurements were available for cortisol, IFN-γ and IL-10, we could calibrate the parameters related to their concentration dynamics, and then update the model in order to explicitly incorporate the dynamical modelling of these quantities using PDEs. Also, our current model does not consider the effects of tumour necrosis and hypoxia or CTL exhaustion. These mechanisms can actively contribute to deregulate the normal levels of pro- and anti-inflammatory cytokines, resulting in more aggressive tumours and impaired immune response [34, 41–43].

From a biological point of view, a natural development of this work would consist in studying the effects of therapeutic strategies which counteract the negative impact of psychological stress on immune infiltration. In fact, in [7] it was found that the administration of glucocorticoid receptor antagonists reversed the effects of cortisol and significantly

enhanced immune infiltration in tumour spheroids. The effects of therapeutic strategies could be incorporated into our model by, for example, including a detailed metabolic network at the sub-cellular level that directly influences the dynamics at the cellular level, such as CTL growth and movement. In this regard, we could also investigate the delivery schedule of therapeutic agents (i.e. time and dosage) that may make it possible to maximise the number of infiltrated CTLs at the end of the treatment.

Despite its relative simplicity, our model provides a novel *in silico* framework to investigate the impact of biological mechanisms linked to psychological stress on immune infiltration, and may be a promising tool to easily and cheaply explore therapeutic strategies designed to increase immune infiltration and improve the overall anti-tumour immune response.

Data availability statement

The data that support the findings of this study are openly available at the following URL/DOI: https://plmlab.math.cnrs.fr/leschiera/roleofstress.

Funding

E L has received funding from the European Research Council (ERC) under the European Union's Horizon 2020 research and innovation programme (Grant Agreement No. 740623). T L gratefully acknowledges support from the the PRIN 2020 Project (No. 2020JLWP23) 'Integrated Mathematical Approaches to Socio-Epidemiological Dynamics' (CUP: E15F21005420006). T L gratefully acknowledge support of the Institut Henri Poincaré (UAR 839 CNRS-Sorbonne Université), and LabEx CARMIN (ANR-10-LABX-59-01). L A, T L and E L gratefully acknowledge support from the CNRS International Research Project 'Modélisation de la biomécanique cellulaire et tissulaire' (MOCETIBI).

ORCID iDs

Emma Leschiera https://orcid.org/0009-0001-3201-1367
Tommaso Lorenzi https://orcid.org/0000-0001-9165-1666
Luis Almeida https://orcid.org/0000-0002-3344-0366

References

[1] Coe C L and Laudenslager M L 2007 Psychosocial influences on immunity, including effects on immune maturation and senescence *Brain Behav. Immunity* **21** 1000–8
[2] Morey J N, Boggero I A, Scott A B and Segerstrom S C 2015 Current directions in stress and human immune function *Curr. Opin. Psychol.* **5** 13–17
[3] Seiler A, Fagundes C P and Christian L M 2020 The impact of everyday stressors on the immune system and health *Stress Challenges and Immunity in Space: From Mechanisms to Monitoring and Preventive Strategies* (Springer) pp 71–92
[4] Lee J W *et al* 2009 Surgical stress promotes tumor growth in ovarian carcinoma *Clin. Cancer Res.* **15** 2695–702
[5] Nilsson M B *et al* 2007 Stress hormones regulate interleukin-6 expression by human ovarian carcinoma cells through a Src-dependent mechanism *J. Biol. Chem.* **282** 29919–26
[6] Budiu R A *et al* 2017 Restraint and social isolation stressors differentially regulate adaptive immunity and tumor angiogenesis in a breast cancer mouse model *J. Clin. Oncol.* **6** 12
[7] Al-Hity G *et al* 2021 An integrated framework for quantifying immune-tumour interactions in a 3D co-culture model *Commun. Biol.* **4** 1–12
[8] Dranoff G 2004 Cytokines in cancer pathogenesis and cancer therapy *Nat. Rev. Cancer* **4** 11–22
[9] Castro F, Cardoso A P, Gonçalves R M, Serre K and Oliveira M J 2018 Interferon-gamma at the crossroads of tumor immune surveillance or evasion *Front. Immunol.* **9** 847
[10] Schiltz P M, Gomez G G, Read S B, Kulprathipanja N V and Kruse C A 2002 Effects of IFN-γ and interleukin-1 β on major histocompatibility complex antigen and intercellular adhesion molecule-1 expression by 9L gliosarcoma: relevance to its cytolysis by alloreactive cytotoxic T lymphocytes *J. Interferon Cytokine Res.* **22** 1209–16
[11] Alhakeem S S, McKenna M K, Oben K Z, Noothi S K, Rivas J R, Hildebrandt G C, Fleischman R A, Rangnekar V M, Muthusamy N and Bondada S 2018 Chronic lymphocytic Leukemia–Derived IL-10 suppresses antitumor immunity *J. Immunol.* **200** 4180–9
[12] Couper K N, Blount D G and Riley E M 2008 IL-10: the master regulator of immunity to infection *J. Immunol.* **180** 5771–7
[13] de Pillis L G and Radunskaya A 2003 A mathematical model of immune response to tumor invasion *Computational Fluid and Solid Mechanics 2003* (Elsevier) pp 1661–8
[14] Kirschner D and Panetta J C 1998 Modeling immunotherapy of the tumor–immune interaction *J. Math. Biol.* **37** 235–52
[15] Kuznetsov V A, Makalkin I A, Taylor M A and Perelson A S 1994 Nonlinear dynamics of immunogenic tumors: parameter estimation and global bifurcation analysis *Bull. Math. Biol.* **56** 295–321
[16] Łuksza M *et al* 2017 A neoantigen fitness model predicts tumour response to checkpoint blockade immunotherapy *Nature* **551** 517–20
[17] Delitala M and Lorenzi T 2013 Recognition and learning in a mathematical model for immune response against cancer *Discrete Contin. Dyn. Syst.* B **18** 891
[18] Kolev M, Nawrocki S and Zubik-Kowal B 2013 Numerical simulations for tumor and cellular immune system interactions in lung cancer treatment *Commun. Nonlinear Sci. Numer. Simul.* **18** 1473–80
[19] Lorenzi T, Chisholm R H, Melensi M, Lorz A and Delitala M 2015 Mathematical model reveals how regulating the three phases of T-cell response could counteract immune evasion *Immunology* **146** 271–80
[20] Atsou K, Anjuère F, Braud V M and Goudon T 2020 A size and space structured model describing interactions of tumor cells with immune cells reveals cancer persistent equilibrium states in tumorigenesis *J. Theor. Biol.* **490** 110163
[21] Atsou K, Anjuère F, Braud V M and Goudon T 2021 A size and space structured model of tumor growth describes a key role for protumor immune cells in breaking equilibrium states in tumorigenesis *PloS One* **16** e0259291
[22] Matzavinos A and Chaplain M A 2004 Travelling-wave analysis of a model of the immune response to cancer *C. R. Biol.* **327** 995–1008
[23] Matzavinos A, Chaplain M A and Kuznetsov V A 2004 Mathematical modelling of the spatio-temporal response of cytotoxic T-lymphocytes to a solid tumour *Math. Med. Biol.* **21** 1–34

[24] Bouchnita A, Belmaati F E, Aboulaich R, Koury M J and Volpert V 2017 A hybrid computation model to describe the progression of multiple myeloma and its intra-clonal heterogeneity *Computation* **5** 16
[25] Ghaffarizadeh A, Heiland R, Friedman S H, Mumenthaler S M and Macklin P 2018 PhysiCell: an open source physics-based cell simulator for 3-D multicellular systems *PLoS Comput. Biol.* **14** e1005991
[26] Almeida L, Audebert C, Leschiera E and Lorenzi T 2022 A hybrid discrete–continuum modelling approach to explore the impact of T-cell infiltration on anti-tumour immune response *Bull. Math. Biol.* **84** 1–37
[27] Leschiera E, Lorenzi T, Shen S, Almeida L and Audebert C 2022 A mathematical model to study the impact of intra-tumour heterogeneity on anti-tumour CD8+ T cell immune response *J. Theor. Biol.* **538** 111028
[28] Christophe C, Müller S, Rodrigues M, Petit A E, Cattiaux P, Dupré L, Gadat S and Valitutti S 2015 A biased competition theory of cytotoxic T lymphocyte interaction with tumor nodules *PLoS One* **10** e0120053
[29] Kather J N *et al* 2017 *In silico* modeling of immunotherapy and stroma-targeting therapies in human colorectal cancer *Cancer Res.* **77** 6442–52
[30] Macfarlane F R, Lorenzi T and Chaplain M A 2018 Modelling the immune response to cancer: an individual-based approach accounting for the difference in movement between inactive and activated T cells *Bull. Math. Biol.* **80** 1539–62
[31] Macfarlane F R, Chaplain M A and Lorenzi T 2019 A stochastic individual-based model to explore the role of spatial interactions and antigen recognition in the immune response against solid tumours *J. Theor. Biol.* **480** 43–55
[32] Izaguirre J A *et al* 2004 CompuCell, a multi-model framework for simulation of morphogenesis *Bioinformatics* **20** 1129–37
[33] Boissonnas A, Fetler L, Zeelenberg I S, Hugues S and Amigorena S 2007 *In vivo* imaging of cytotoxic T cell infiltration and elimination of a solid tumor *J. Exp. Med.* **204** 345–56
[34] Galon J and Bruni D 2019 Approaches to treat immune hot, altered and cold tumours with combination immunotherapies *Nat. Rev. Drug Discovery* **18** 197–218
[35] Gorbachev A V, Kobayashi H, Kudo D, Tannenbaum C S, Finke J H, Shu S, Farber J M and Fairchild R L 2007 CXC chemokine ligand 9/monokine induced by IFN-γ production by tumor cells is critical for T cell-mediated suppression of cutaneous tumors *J. Immunol.* **178** 2278–86
[36] Tokunaga R, Zhang W, Naseem M, Puccini A, Berger M D, Soni S, McSkane M, Baba H and Lenz H-J 2018 CXCL9, CXCL10, CXCL11/CXCR3 axis for immune activation–a target for novel cancer therapy *Cancer Treat. Rev.* **63** 40–47
[37] Harjunpää H, Llort Asens M, Guenther C and Fagerholm S C 2019 Cell adhesion molecules and their roles and regulation in the immune and tumor microenvironment *Front. Immunol.* **10** 1078
[38] Jorgovanovic D, Song M, Wang L and Zhang Y 2020 Roles of IFN-γ in tumor progression and regression: a review *Biomark Res.* **8** 1–16
[39] Cronstein B N, Kimmel S C, Levin R I, Martiniuk F and Weissmann G 1992 A mechanism for the antiinflammatory effects of corticosteroids: the glucocorticoid receptor regulates leukocyte adhesion to endothelial cells and expression of endothelial-leukocyte adhesion molecule 1 and intercellular adhesion molecule 1 *Proc. Natl Acad. Sci.* **89** 9991–5
[40] Kalfeist L, Galland L, Ledys F, Ghiringhelli F, Limagne E and Ladoire S 2022 Impact of glucocorticoid use in oncology in the immunotherapy era *Cells* **11** 770
[41] Balkwill F 2009 Tumour necrosis factor and cancer *Nat. Rev. Cancer* **9** 361–71
[42] Jiang Y, Li Y and Zhu B 2015 T-cell exhaustion in the tumor microenvironment *Cell Death Dis.* **6** e1792–2
[43] Wherry E J 2011 T cell exhaustion *Nat. Immunol.* **12** 492–9